Inorg. Chem. **1992**, *31*, 4697–4699 **4697**

Notes

Electrochemistry of Planar Cobalt(II) and Nickel(II) Tetraaza[14]annulene Complexes

Peter J. Lukes, Alan C. McGregor, Thomas Clifford, and Joe A. Crayston*

Department of Chemistry, University of St. Andrews,
St. Andrews, Fife, Scotland KY16 9ST

Received May 1, 1991

Introduction

Electrochemical studies of tetraaza[14]annulene[1] complexes have relevance to designing both catalysts (for dioxygen binding, for example)[2] and new materials (e.g. electrochromics and conducting polymers).[3] The redox potentials can be tuned over a wide potential range by variations in ring size, substituents, degree of unsaturation, conjugation around the ring, and the charge on the ligand.[4,5] However, the simple dibenzotetraazaannulenes, e.g. H_2[dibenzo[14]tetraene]N_4 (or TADA-H_2, **1**) have low solubility in electrochemical solvents. The related macrocycle H_2[Me_5dibenzo[14]tetraene]N_4 **2**[6,7] while having considerably greater solubility due to its nonplanar structure arising from the steric interactions between the methyl substituents and the ortho protons on the benzene rings, undergoes undesirable side reactions. Thus the solution electrochemistry of the Ni,[8] Co[9] and Cu[8] complexes of **2** is complicated by oxidatively induced dimerization and film formation.[10–13] Ligand **2** and its complexes may well be a special case in the tetraazaannulenes series since they are not planar, but saddle-shaped. In this paper we describe Co^{II} and Ni^{II} complexes of the new ligands H_2[Me_2dibenzo[14]tetraene]N_4 (**3**), H_2[Me_2ditol[14]tetraene]N_4 (**4**), and H_2[Me_2dixyl[14]tetraene]N_4 (**5**), which have been shown to be planar by X-ray crystallography.[14,15] These ligands also have the advantage of bridgehead substituents (i.e. at the 6,13-positions) which have been shown to hinder coupling reactions.[16,17] The stability of the complexes permits a study of the effect of axial base on the $Co^{III/II}$ and $L^{+/0}$ couples of tetraazaannulenes. The electrochemical data may be used to predict the band maxima of observed ligand to metal charge transfer bands in the visible spectra of these complexes.

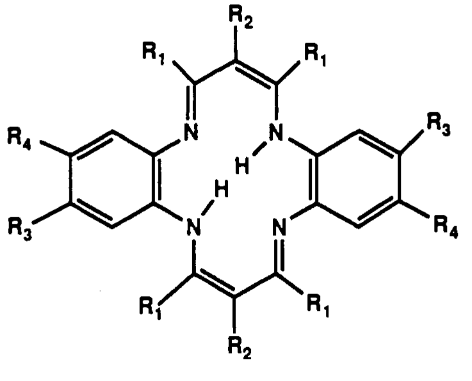

1	$R_1, R_2, R_3, R_4 = H$	H_2[dibenzo[14]tetraene]N_4
2	$R_1 = CH_3$; $R_2, R_3, R_4 = H$	H_2[Me_5dibenzo[14]tetraene]N_4
3	$R_2 = CH_3, R_1, R_3, R_4 = H$	H_2[Me_2dibenzo[14]tetraene]N_4
4	$R_1 = H$; $R_2 = CH_3$; R_3 or $R_4 = CH_3$	H_2[Me_2ditol[14]tetraene]N_4
5	$R_1 = H$; $R_2 = CH_3$; $R_3 = R_4 = CH_3$	H_2[Me_2dixyl[14]tetraene]N_4

Experimental Section

Physical Measurements. UV–visible spectra in the 350–850-nm range were measured on a Philips PU8720 spectrometer. Cyclic voltammograms were recorded using a three-electrode cell comprising a Pt-disk working electrode (area = 2×10^{-3} cm^2), a Pt-wire auxiliary electrode, and a saturated calomel reference electrode. The potentiostat was a Pine Instruments RDE4, and this was coupled to a Graphtec WX2300 X-Y recorder. The supporting electrolyte, tetra-*n*-butylammoniumhexafluorophosphate (TBAHFP) was recrystallized prior to use. Solvents (CH_2Cl_2, HPLC grade, and DMF) used in the electrochemical experiments were obtained from Aldrich and were distilled prior to use; spectroscopic grade solvents were used as received. The solvent of choice for the study of the electrochemical properties of this group of macrocyclic compounds is DMF, for although the anodic limit of this solvent is lower than that of other electrochemical solvents, the compounds dissolve readily and are less prone to the precipitation which we believe to be the cause of many of the complications in the voltammetry of these species.

The synthesis of the ligands and their metal complexes employed a condensation reaction between 3-ethoxy-2-methylacrolein (Fluka) and 1,2-diaminobenzene (Aldrich) in dimethylformamide (DMF) to give **3**,[18] 1,2-diamino-5-methyl benzene (Aldrich) to give **4**, and 1,2-diamino-4,5-dimethylbenzene (Aldrich) to give **5**. Recrystallization from DMF yields samples of the ligand and complexes for which C, H, and N analyses were within 2% of calculated values.

Results and Discussion

Cobalt Complexes. Comparison of the positions of the redox waves observed in the cyclic voltammogram of Co(**4**) in DMF (Figure 1a) with those of the uncomplexed ligand (Table I) clearly allows assignment of the $Co^{III/II}$ couple at +0.17 V vs SCE. The effect of an axially-coordinated base on the position of the $Co^{III/II}$ couple is of particular interest and has hitherto not been investigated for this class of compounds. As shown in Figure 1b, coordination of pyridine by the complex Co(**4**) shifts the potential

---

(1) Melson, G. A. *Coordination Chemistry of Macrocyclic Compounds*; Plenum Press: New York, 1979.

(2) Niederhoffer, E. C.; Timmons, J. H.; Martell, A. E. *Chem. Rev.* **1984**, *84*, 137.

(3) (a) Hanack, M.; et al. *Handbook of Conducting Polymers*; Marcel Dekker Inc.: New York, 1986; pp 113–205. (b) Honeybourne, C. L. *J. Phys. Chem. Solids* **1987**, *48*, 109–141.

(4) Lindoy, L. F. *The Chemistry of Macrocyclic Ligand Complexes*; Cambridge University Press: Cambridge, U.K., 1989; pp 209–223.

(5) Busch, D. H. *Acc. Chem. Res.* **1978**, *11*, 392.

(6) Goedken, V. L.; Weiss, M. C. *Inorg. Synth.* **1980**, *20*, 115.

(7) The related tetraphenyl derivative has recently been reported: Hochgesang, P. J.; Bereman, R. D. *Inorg. Chim. Acta* **1989**, *162*, 191.

(8) Bailey, C. L.; Bereman, R. D.; Rillema, D. P.; Nowak, R. *Inorg. Chem.* **1984**, *23*, 3956.

(9) Bailey, C. L.; Bereman, R. D.; Rillema, D. P. *Inorg. Chem.* **1986**, *25*, 3149.

(10) McElroy, F. C.; Dabrowiak, J. C. *J. Am. Chem. Soc.* **1976**, *98*, 7112.

(11) Bailey, C. L.; Bereman, R. D.; Rillema, D. P.; Nowak, R. *Inorg. Chem.* **1986**, *25*, 933.

(12) Hochgesang, P. J.; Bereman, R. D. *Inorg. Chim. Acta* **1990**, *167*, 199.

(13) Kadish, K. M.; Schaeper, D.; Bottomley, L. A.; Tsutsui, M.; Bobsein, R. L. *J. Inorg. Nucl. Chem.* **1980**, *42*, 469–474.

(14) Lukes, P. J.; Crayston, J. A.; Ando, D. J.; Harman, M. E.; Hursthouse, M. B. *J. Chem. Soc., Perkin Trans. 2* **1991**, 1845.

(15) Sister, E.; Gottfried, V.; Kapon, M.; Kaftory, M.; Dori, Z.; Gray, H. B. *Inorg. Chem.* **1988**, *27*, 600.

(16) Abelleira, A.; Walsh, F. *Electrochim. Acta* **1986**, *31*, 113.

(17) Dabrowiak, J. C.; Fisher, D. P.; McElroy, F. C.; Macero, D. J. *Inorg. Chem.* **1979**, *18*, 2304.

(18) After this work was completed we became aware of previously reported syntheses of **3–5** using our method: (a) Lorch, E.; Breitmaier, E. *Chem.-Ztg.* **1975**, *99*, 87. (b) Asahi Chemical Industry Co., Ltd. *Jpn. Kokai Tokkyo Koho* JP 58 38,272 [83 38272], 1983; *Chem. Abstr.* **1983**, *99*, 22510n. (c) Yatluk, Y. G.; Suvorov, A. L. *Khim. Geterotsikl. Soedin.* **1987**, 376; *Chem. Abstr.* **1988**, *108*, 21863x. (d) Makin, S. M.; Broido, P. I.; Pomogaev, A. I.; Nikulina, S. A. *Khim. Geterotsikl. Soedin.* **1989**, 103; *Chem. Abstr.* **1989**, *111*, 32664w. (e) Davies, D. L. University of Leicester. Private communication.

0020-1669/92/1331-4697$03.00/0

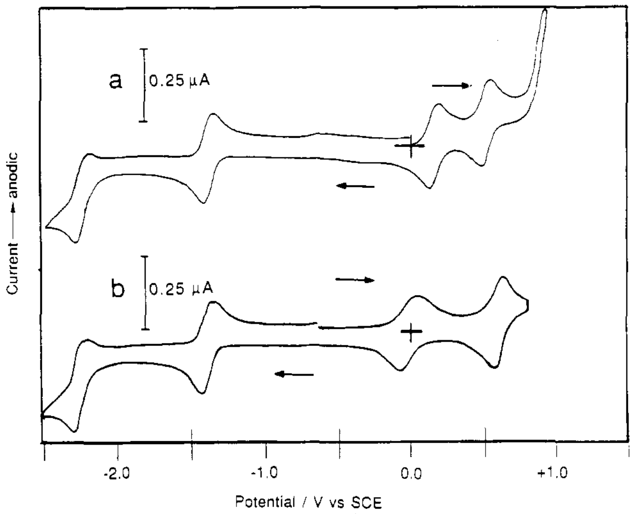

Figure 1. (a) Cyclic voltammogram (100 mV s^{-1}) of Co[Me$_2$diTol[14]-tetraene]N$_4$. The anodic limit of the scan was chosen to avoid complications from the L/L$^+$ oxidation. (b) Voltammogram after addition of a stoichiometric quantity of pyridine (Pt electrode, 0.1 mol dm^{-3} TBAHFP in DMF).

Table I. Redox Potentials (V) of Tetraazaannulene Ligands and Complexes in DMF

compd	$L^{0/-}$	$M^{II/I}$	$M^{III/II}$	$L^{+/0}$	$L^{2+/+}$
1, TAA	-1.77^c			0.75^a	1.06^a
2, TMTAA	-2.25^c			0.79^a	0.95^a
(2)Ni^b		-1.73 (60)		0.45^a	1.00^a
(2)Co^b		-1.65 (90)	0.01 (60)	0.55 (60)	1.04 (60)
3	-1.85^c			0.64^a	0.98^a
4	-1.85^c			0.55^a	0.85^a
(4)Ni		-1.75 (60)	0.42 (70)	0.63 (50)	1.01 (60)
(4)Co	-2.25 (70)	-1.39 (70)	0.17 (60)	0.53 (60)	0.91^a

[a] E_{pa} only. [b] Data from ref 9, with MeCN as solvent. [c] E_{pc} only. Figures in parentheses are peak separations in mV. Scan rate = 100 mV/s, Pt working and counter electrodes, SCE reference electrode, ferrocene standard (Fc/Fc+ = 0.49 V).

Table II. Observed and Calculated Charge-Transfer Band Positions Based on Electrochemical Data^a

compd	obsd band max/nm	calcd band max/nm
(1)H$_2$	437, 418	441^{b,c}
(2)H$_2$	429, 382	428,^{b} 399^b
(2)Co	578, 536, 541, 411	564^{c-e}
(2)Ni	583	585^d
(2)Pd	490, 415	544^{c,d,f}
(2)Cu	630, 408	648^{c-e}
(3)H$_2$	453, 382	451^b
(4)H$_2$	456, 437, 386	c,420^{b,c}
(4)Co	608, 532, 435, 425, 385	646,^{d} 537,^{d} 446,^{b,c} 392^b
(4)Ni	532, 446, 426	521,^{d} 446^{b,c}

[a] λ (nm) = 1240/ΔE(eV), all calculated data based on data in Table I (this work), unless otherwise stated. Only low-energy bands >375 nm considered. [b] IL (intraligand) π-π^* band: ΔE(eV) = $E(L^{0/+}) - E(L^{0/-})$. [c] Insufficient electrochemical data. [d] LMCT (ligand to metal charge-transfer) band: ΔE(eV) = $E(L^{0/+}) - E(M^{2+/+})$. [e] Reference 9. Electrochemical data recorded in CH$_2$Cl$_2$. [f] Electrochemically irreversible reduction peak prevents use of $E°$ data in calculations.

of this couple to a more negative potential by 140 mV. At the same time the visible spectrum changes dramatically with a prominent new band appearing at λ_{max} 486 nm (Table II). In similar complexes this change has been interpreted as being due to the formation of a monopyridine adduct.[19] Coordination of a molecule of pyridine at an axial site results in a change in the ground state of the complex so that the metal-based HOMO is no longer a d_{xy} orbital but is replaced by a d_{z^2} orbital of higher energy, and hence the oxidation potential of the Co$^{III/II}$ couple is lowered. This effect is also communicated to the first oxidation potential of the ligand, which is shifted with respect to the value obtained in the absence of pyridine, though the shift this time is smaller (70 mV) and toward a more positive value, making the ligand more difficult to oxidize. The raising of the oxidation potential of the ligand in the presence of pyridine results from π-bonding competition between pyridine and the macrocycle. Pyridine acts as a π-acceptor, thus reducing the metal–ligand π-bonding and raising the oxidation potential of the ligand. The Co$^{II/I}$, L/L$^-$, and L^{2+}/L$^+$ potentials, however, remain unchanged.

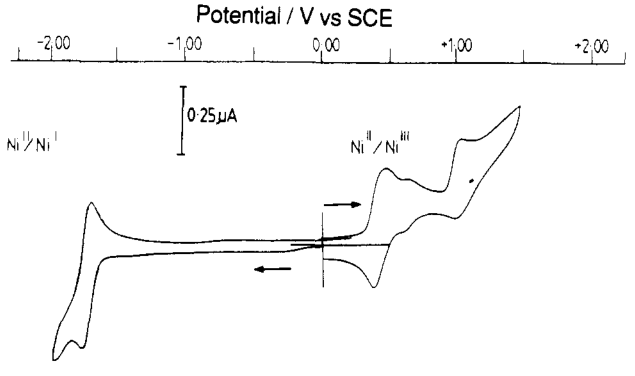

Figure 2. Cyclic voltammogram (100 mV s^{-1}) of Ni[Me$_2$diTol[14]-tetraene]N$_4$ (Pt electrode, 0.1 mol dm^{-3} TBAHFP in DMF).

Imidazole also lowers the reduction potential of the Co$^{III/II}$ couple. When imidazole is present in a stoichiometric (1:1) quantity, the couple is found at −0.24 V, a shift of 410 mV. This large shift may be interpreted as a large formation constant for the pyridine complex. Interestingly, the first ligand oxidation potential is *also* shifted to a more negative potential (+0.35 V) after adding imidazole. Imidazole is a good π-donor[20] and will thus increase the electron density available on the metal for back-donation to the ligand. In so doing the potential of the *ligand* oxidation is lowered. No direct correlation exists between pK_a and the redox potentials for this group of structurally unrelated bases. In a series of related ligands the negative shift of the ligand redox potential should be a measure of the tendency of the complex to bind O$_2$. A less electronegative ligand will permit strong Co–O$_2$ bonds to be formed.[21]

For the group of related Co complexes Co(**3**), Co(**4**), and Co(**5**) the Co$^{II/I}$ couple follows the order **5** < **4** < **3**; i.e., the reduction potential is more negative for the most highly methyl substituted (electron rich) macrocycle. The Co$^{III/II}$, and L$^{+/0}$ couples do not, however, follow any definite order (Table I). The large peak separation of the Co$^{III/II}$ couple (340 mV) in the complex Co(**3**) indicates an electrochemically irreversible couple (slow electron transfer), and makes an accurate determination of the E^0 value difficult. This also precludes detailed comparison of its position and those of the Co$^{III/II}$ couples in Co(**4**) and Co(**5**). The irreversible behavior probably arises from differing coordination about the Co center in the II, III oxidation states as observed for pyridine coordination to cobalt porphyrins, where two pyridines coordinate in the Co^{III} state, one more than for the Co^{II} state.[22]

Nickel. Cyclic voltammetry of Ni(**4**) in DMF (Figure 2) reveals waves for both the Ni$^{III/II}$ and Ni$^{II/I}$ couples. If we consider the d-orbitals involved in the Ni^{II} oxidation in the Ni macrocycle the oxidation of the central metal to the Ni^{III} state is facilitated by the strong in-plane interaction which raises the energy of the $d_{x^2-y^2}$ orbital, the so-called redox orbital. For square-planar Ni^{II} compounds of tetraaza macrocycles the potential range for the Ni$^{III/II}$ couple spans over 2 V, with the position being influenced

---

(19) Sakata, K.; Hayashida, Y.; Hashimoto, M.; Terada, K.; Kato, Y. *Inorg. Chim. Acta* **1983**, *105*, L25.

(20) Stynes, D. V.; Stynes, H. C.; James, B. R.; Ibers, J. A. *J. Am. Chem. Soc.* **1973**, *95*, 1796.

(21) Carter, M. J.; Rillema, D. P.; Basolo, F. *J. Am. Chem. Soc.* **1974**, *96*, 392.

(22) Kadish, K. M. *Prog. Inorg. Chem.* **1986**, *34*, 435–605.

by both ring size and the strength of the in-plane interactions. The position of the couple observed in this work is in accord with expectations based on a comparison of ring size and the degree of conjugation around the ring once the effects of solvent and reference electrode have been accounted for.[4,5] The failure to observe the $Ni^{III/II}$ couple in voltammograms of Ni(**2**) is due to the smaller in-plane interactions resulting from the buckled ligand (**2**), driving the couple to more positive potentials.

Visible Spectroscopy. Visible spectra of the free ligands **3**–**5** and their Ni and Co complexes were recorded in DMF and are in accord with literature data on *planar* tetraazaannulene complexes (Table II). The spectra of the saddle-shaped ligand (**2**) and its complexes are quite different.[8,9] The bands which appear after complexation, at 530 and 600 nm, are of the ligand to metal charge-transfer (LMCT) variety since they are too intense to be d–d transitions. It is possible to estimate the energies of these transitions very simply from the difference in redox potentials for ligand oxidation and metal reduction, as has been attempted for metal porphyrins[23] and phthalocyanines.[24] The complexes studied in this work seem particularly promising for this analysis: they have a rich and well-understood electrochemistry, and the visible region of the spectrum is uncluttered by intraligand absorptions. Using the data of Table I in

$$\Delta E(\mathrm{LMCT}) \sim E(\mathrm{L/L^+}) - E(\mathrm{M^{2+/+}}) \qquad (1)$$

where $E(\mathrm{L/L^+})$ is the redox potential for oxidation of the ligand and $E(\mathrm{M^{2+/+}})$ is the redox potential for reduction of the metal, we may estimate the positions of the LMCT transitions in eV, ΔE(LMCT), as shown in Table II. Within the limitations of the reliability of the electrochemical data, the agreement in band position is quite striking. Less convincing, however, is the ability to predict the precise number of bands; this is largely due to the lack of complete electrochemical data for compounds not studied under the ideal conditions outlined in this paper. Several observations on the data may be made. First, the planar ligands appear to be more easily oxidized than **2** (probably because the charge may be delocalized); this means that the intraligand bands are of lower energy in the free ligands. However, when the ligands are complexed the ligand redox potentials become comparable. Since the planar ligands seem to stabilize the lower oxidation states of Co more than the nonplanar ligand **2** (the complexes are easier to reduce, Table I), the LMCT bands occur at slightly lower energy. The situation is less clear for the Ni^{II} complexes due to uncertainty in the reversible potentials of Ni(**2**); however, here it seems that **2** slightly favors the lower oxidation state Ni^{I}, leading to a lower energy LMCT band.

Conclusions

The planar, bridgehead-substituted complexes stabilize the Co^{I} oxidation state. A cyclic voltammetry study of axial base coordination has revealed fundamental differences between the two bases, pyridine and imidazole. This is clear evidence for the participation of metal d_{xz} and d_{yz} orbitals in both metal–ligand and metal–base interactions.

Acknowledgment. We thank SERC for support, and Prof. R. W. Hay for stimulating discussions.

Supplementary Material Available: Figures showing UV–visible spectra and NMR spectra and a table of NMR spectroscopic data (4 pages). Ordering information is given on any current masthead page.

Registry No. **1**, 22119-35-3; (**1**)$^-$, 72345-96-1; (**1**)$^+$, 72298-56-7; (**1**)$^{2+}$, 143680-05-1; **2**, 56276-51-8; (**2**)$^-$, 72345-97-2; (**2**)$^+$, 72298-57-8; (**2**)$^{2+}$, 143680-06-2; (**2**)Co, 60193-64-8; (**2**)Ni, 51223-51-9; (**2**)Pd, 68833-19-2; (**2**)Cu, 56285-38-2; **3**, 55424-75-4; (**3**)$^-$, 143618-18-2; (**3**)$^+$, 143680-07-3; (**3**)$^{2+}$, 143680-08-4; **4**, 143618-19-3; (**4**)$^-$, 143728-44-3; (**4**)$^+$, 143618-20-6; (**4**)$^{2+}$, 143680-09-5; (**4**)Ni, 105194-86-3; [(**4**)Ni]$^-$, 143594-04-1; [(**4**)Ni]$^+$, 143594-03-0; (**4**)Co, 50928-50-2; [(**4**)Co]$^-$, 143594-02-9; [(**4**)Co]$^+$, 143593-97-9; (**4**)Co·pyridine, 143593-99-1; [(**4**)Co·pyridine]$^+$, 143593-98-0; (**4**)Co·imidazole, 143594-00-7; [(**4**)Co·imidazole]$^+$, 143594-01-8; DMF, 68-12-2; pyridine, 110-86-1; imidazole, 288-32-4.

---

(23) Gouterman, M.; Hanson, L. K.; Khalil, G.-E.; Leenstra, W. R.; Buchler, J. W. *J. Chem. Phys.* **1975**, *62*, 2343.

(24) Lever, A. B. P.; Pickens, S. R.; Minor, P. C.; Licoccia, S.; Ramaswamy, B. S.; Magnell, K. *J. Am. Chem. Soc.* **1981**, *103*, 6800.